STEM CELLS AND DEVELOPMENT
Volume 25, Number 8, 2016

DOI: 10.1089/scd.2015.0356

Soft Elasticity-Associated Signaling and Bone Morphogenic Protein 2 Are Key Regulators of Mesenchymal Stem Cell Spheroidal Aggregates

Zoe Cesarz,[1] Jessica L. Funnell,[1,*] Jianjun Guan,[2] and Kenichi Tamama[1,3]

Cell therapy with adult mesenchymal stem cells (MSCs) is a promising approach to regenerative medicine and autoimmune diseases. There are various approaches to improve the efficacy of MSC-based therapeutics, and MSC preparation as spheroidal aggregates, or MSC spheroids, is a novel preparatory and delivery method. Spheroid formation induces a dramatic change in the gene expression profile of MSCs. Self-activation of interleukin-1 (IL1) signaling was shown to be upstream of both pro- and anti-inflammatory genes in MSC spheroids, but the molecular pathways that initiate IL1 signaling remain unknown. As bone morphogenic protein *(BMP)2* upregulation precedes that of *IL1B* expression during spheroid formation, we hypothesized that BMP2 signaling triggers IL1 signaling in MSC spheroids. Contrary to expectations, BMP2 signaling decreased expression of *IL1B* and downstream genes in a SMAD6-dependent manner. Conversely, IL1B signaling enhanced *BMP2* expression. Another major difference between two-dimensional (2D) monolayer culture and three-dimensional (3D) spheroid culture is the Young's elasticity modulus, or stiffness, of the materials surrounding the cells, as there is a million-fold difference between a plastic surface for standard 2D culture (GPa) and 3D spheroidal aggregates (0.1 kPa). We tested another hypothesis that soft elasticity-associated mechanosignaling initiates the gene expression change during spheroid formation. Results showed that both *BMP2* expression and inflammatory signaling are upregulated in an elasticity-associated signaling-dependent manner in MSCs. Lastly, BMP2 signaling enhanced cell survival and cell spreading of MSC spheroids. In summary, our study suggests that soft elasticity and BMP2 signaling are critical for MSC spheroids.

Introduction

Cell therapy with adult mesenchymal stem cells (MSCs) is a promising approach in the field of regenerative medicine and autoimmune diseases [1–3]. There are various approaches to improve the efficacy of MSC-based therapeutics [4]. MSC preparation as three-dimensional (3D) spheroidal aggregates or MSC spheroids is a novel preparatory and delivery method, as summarized in our latest review article [5]. Spheroid formation enhances anti-inflammatory and angiogenic effects of MSCs, leading to improvement in their overall therapeutic potential [6–9]. Spheroid formation also improves MSC stemness [7,10,11] and causes dramatic changes in the gene expression profile (eg, upregulation of pro- and anti-inflammatory mediators) of MSCs as compared with standard two-dimensional (2D) monolayer MSC culture [12]. Moreover, the 3D condition provides the stem cell niche and organogenesis microenvironment in the body and thus, the 3D cell culture system should also provide better understanding of the molecular mechanisms that regulate stem cell behavior in both native and bio-engineered tissues [13]. A recent article proposes MSC spheroids as an in vitro model of blastemas, cellular aggregates of undifferentiated cells capable of tissue repair and regeneration [14].

Self-activation of caspase and subsequent activation of interleukin-1 (IL1) signaling were shown to be upstream events of proinflammatory cytokines and anti-inflammatory molecules, such as tumor necrosis factor, alpha-induced protein 6/tumor necrosis factor-inducible gene 6 (TNFAIP6/TSG6) in MSC spheroids [15]. One potential upstream event that activates caspase is the alteration of mitochondrial bioenergetics in MSC spheroids [16], but those results cannot account for the overall change in the gene expression profile in MSC spheroids. This unique characteristic should be responsible for the enhanced therapeutic potential of MSC spheroids through augmented production of bioactive molecules, such as

[1]Department of Pathology, University of Pittsburgh School of Medicine, Pittsburgh, Pennsylvania.
[2]Department of Materials Science and Engineering, the Ohio State University, Columbus, Ohio.
[3]McGowan Institute for Regenerative Medicine, University of Pittsburgh, Pittsburgh, Pennsylvania.
*Current affiliation: Binghamton University, State University of New York, Watson School of Engineering, Binghamton, New York.

Table 1. TaqMan© Probes/Primers Used in This Article

ACTA2	actin, alpha 2, smooth muscle, aorta	Hs00426835_g1
ACTB	actin, beta	Hs01060665_m1
BMP2	bone morphogenic protein 2	Hs00154192_m1
IL1B	interleukin 1 beta	Hs01555410_m1
IL8	interleukin 8	Hs00174103_m1
LIF	leukemia inhibitory factor	Hs00171455_m1
PTGS2/COX2	prostaglandin-endoperoxidase synthase 2/cyclooxygenase-2	Hs00153133_m1
SMAD6	SMAD family member 6	Hs00178579_m1
SOD2	superoxide dismutase 2, mitochondrial	Hs00167309_m1
TNFAIP6	tumor necrosis factor, alpha-induced protein 6	Hs01113602_m1

cytokines, but the underlying molecular mechanisms upstream of IL1 signaling self-activation and the massive change of gene expression profile remain obscure.

Bone morphogenic proteins (BMPs) are pleiotropic morphogens and cytokines that belong to the transforming growth factor-β (TGF-β) family. Originally isolated as bone matrix-derived bioactive factors that cause ectopic bone formation, BMPs and their antagonists, such as Noggin, have been shown to be involved in embryogenesis; namely, gastrulation, mesoderm induction, dorsal–ventral patterning, organogenesis, limb bud chondrogenesis, and bone morphogenesis [17]. Moreover, BMP signaling was shown to induce regenerative and morphogenic responses in mammalian digits of neonatal mice through blastema formation [18]. The cells forming blastemas are believed to be MSCs [19].

As we show later, *BMP2* is among the most upregulated genes in MSC spheroids. Although the role of BMP2 has been studied extensively in MSC biology in the context of osteogenesis or osteoblastic differentiation [20], the exact role of BMP2 signaling in MSC spheroids remains unknown. Because of strong *BMP2* induction upon formation of MSC spheroids and the key role of BMP signaling in blastema formation, we hypothesized that BMP2 signaling plays a regulatory role in MSC spheroids. Specifically, BMP2 signaling was hypothesized to be upstream of IL1 activation in MSC spheroids.

Another major difference between 2D monolayer culture and 3D spheroid culture is the Young's elasticity modulus, or stiffness, of the materials surrounding the cells, as it reaches to more than a million-fold difference between the plastic surface and the surface of 3D spheroidal aggregates of MSCs [21]. Elasticity of the matrix surrounding the cell is a strong determinant of gene expression and cell differentiation [22], and thus, we formulated a second hypothesis that soft elasticity-associated mechano-signaling functions as a regulatory mechanism in the early phase of spheroid formation.

In this study, we will show that BMP2 signaling is inhibitory for IL1 signaling in MSC spheroids, contrary to our initial expectation. We will also show that soft elasticity-associated mechano-signaling is another key signaling pathway that contributes to the dramatic gene expression profile change in MSC spheroids.

Materials and Methods

This study was approved by the University of Pittsburgh Institutional Biosafety Committee for recombinant DNA research and biohazard agents in accordance with the National Institutes of Health Guidelines for Research involving Recombinant DNA molecules.

Materials

Minimal essential medium α (MEMα), Dulbecco's modified Eagle's medium (DMEM), and all reagents for polymerase chain reaction (PCR) were purchased from Thermo Fisher Scientific. Fetal bovine serum (FBS) was

Table 2. Upregulated and Downregulated Genes and Their Fold-Change in MSC Spheroids as Compared with MSCs in 2D Standard Culture in Fig. 1

Upregulated genes			*Downregulated genes*		
IL1A	Interleukin 1, alpha	36.76	*CTGF*	Connective tissue growth factor	−11.53
BMP2	Bone morphogenetic protein 2	17.27	*ACTB*	Actin, beta	−7.79
IL1B	Interleukin 1, beta	9.76	*SERPINE1*	Serpin peptidase inhibitor, clade E, member 1	−6.35
CXCL2	Chemokine (C-X-C motif) ligand 2	8.24	*COL4A1*	Collagen, type IV, alpha 1	−5.77
PTGS2/COX2	Prostaglandin-endoperoxide synthase 2/cyclooxygenase-2	7.93	*DKK1*	Dickkopf homolog 1 (Xenopus laevis)	−5.17
EREG	Epiregulin	6.77	*ITGA6*	Integrin, alpha 6	−5.09
IL11	Interleukin 11	5.90	*ACTA2*	Actin, alpha 2, smooth muscle, aorta	−4.75
CXCL1	Chemokine (C-X-C motif) ligand 1	4.93	*PDGFA*	Platelet-derived growth factor alpha	−4.16
BMP6	Bone morphogenetic protein 6	3.05	*COL1A1*	Collagen, type I, alpha 1	−4.06
VEGFA	Vascular endothelial growth factor A	2.98	*TAGLN*	Transgelin	−3.33
ITGA2	Integrin, alpha 2	2.93	*COL5A1*	Collagen, type V, alpha 1	−2.99
SPP1	Secreted phosphoprotein 1	2.71	*VEGFC*	Vascular endothelial growth factor C	−2.87
			COL1A2	Collagen, type I, alpha 2	−2.78
			ANGPT1	Angiopoietin 1	−2.77
			PDGFC	Platelet-derived growth factor C	−2.68

These genes are all upregulated or downregulated in MSC spheroids in the microarray data already published by Potopova et al. [12].
MSC, mesenchymal stem cell; qRT-PCR, quantitative reverse transcription–polymerase chain reaction.

purchased from Atlanta Biologicals. SP600125 (JNK inhibitor) was purchased from EMD Millipore. Soft elasticity cell culture plates with 200 Pa surface were purchased from Advanced BioMatrix. Human recombinant BMP2 was purchased from Bio-Techne. Human recombinant IL1B was purchased from Peprotech. TPCA-1 (IκB kinase-2 inhibitor) was purchased from Sigma-Aldrich.

Cell culture

Human primary bone marrow MSCs (prhMSCs) were purchased from Lonza (Basel, Switzerland) and cultured in MEMα supplemented with 17% FBS, 2 mM L-glutamine, 1 mM pyruvate, 100 μM nonessential amino acids, and 100 U/mL penicillin–streptomycin. Immortalized human bone marrow MSCs (imhMSCs) (another donor derived, obtained from Lonza) were generously gifted by Dr. Junya Toguchida (Kyoto University, Japan) [23]. These cells were cultured in DMEM supplemented with 10% FBS, 2 mM L-glutamine, 1 mM pyruvate, 100 μM nonessential amino acid, and 100 U/mL penicillin–streptomycin (Thermo Fisher Scientific). Multipotency of prhMSCs and imhMSCs used in this study was validated previously [24,25].

The soft elasticity plates were coated with Rat Tail Collagen Type 1 (Sigma-Aldrich) before culture as per manufacturer's instruction. Briefly, 2 mL of 100 μg/mL collagen was incubated in each well at room temperature for 1 h. Collagen solution was removed and rinsed with phosphate-buffered saline, and then cells were immediately seeded for experimental use.

3D spheroid culture

MSCs were suspended in 10 μL hanging drops of standard media at a concentration of 1,000 cells/μL (10,000 cells in total) on an inverted cell culture lid, as reported previously [26]. Drops were maintained at 37°C, 5% CO_2 for 12–72 h. All exogenous stimulation and inhibitors were applied during suspension.

Histology

For histological studies, MSC spheroids were encapsulated with 1% agar and fixed immediately with 10% formalin; then, the formalin-fixed paraffin-embedded sections including MSC spheroids were stained with hematoxylin-eosin or fluorescent phalloidin for F-actin staining.

Quantitative reverse transcription–polymerase chain reaction and PCR array

mRNA transcripts were quantified by two-step quantitative reverse transcription–polymerase chain reaction (qRT-PCR) using the TaqMan© PCR system (Thermo Fisher Scientific) or PCR arrays (Qiagen). The quantitative real-time PCR thermal cycler, Mx3005P (Stratagene), was utilized, as described previously [27,28].

TaqMan PCR primers are listed in Table 1. Total RNA was harvested using PureLink RNA Mini Kit with on-column DNase digestion, according to manufacturer's instructions. cDNA was synthesized using High Capacity RNA-to-cDNA kit, then mixed with TaqMan Fast Gene Expression Mastermix and each TaqMan gene-specific primer for the following PCR reaction: 95°C for 20 s, then 40 cycles of 95°C for 1 s, 60°C for 20 s with fluorescence readings taken after each cycle. Total cDNA, as assessed by Qubit ssDNA Assay Kit, was used for normalization [5].

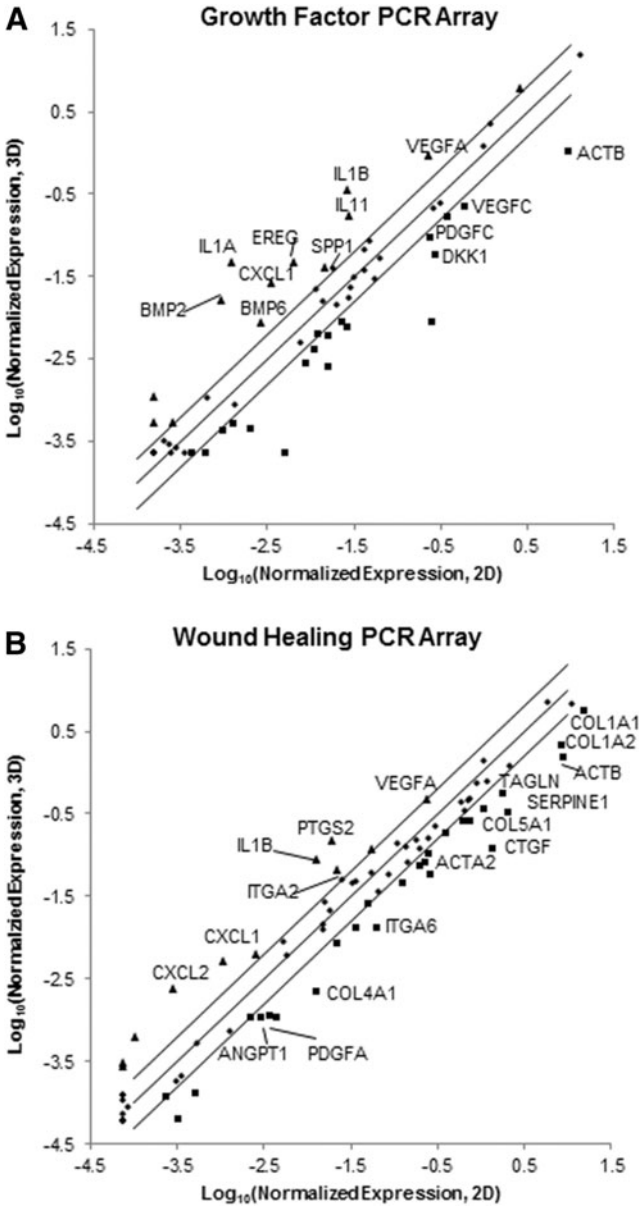

FIG. 1. Comparison of gene expression profile between 2D standard culture and 3D spheroidal culture by PCR Array. MSC spheroids were prepared using the hanging drop method for 48 h and total RNA was harvested for gene expression analysis by qRT-PCR with Human Growth Factor PCR Array **(A)** or Human Wound Healing PCR Array (Qiagen) **(B)**. The relative expression levels for each gene in the 2D standard culture (*x*-axis) and 3D spheroid culture (*y*-axis) samples are plotted against each other in the scatter plot. The upregulated genes (>2) are shown with *triangles*, whereas the downregulated genes (<0.5) are shown with *squares*. 2D, two-dimensional; 3D, three-dimensional; qRT-PCR, quantitative reverse transcription–polymerase chain reaction; MSC, mesenchymal stem cell.

The Human Growth Factor and Wound Healing RT^2 Profiler™ PCR Arrays (Qiagen) were used for profile expression of 86 genes each (Supplementary Tables S1 and S2; Supplementary Data are available online at www.liebertpub.com/scd), according to manufacturer's instructions. In brief, after total RNA was harvested and DNase digested, as stated above, cDNA was synthesized with the RT^2 First Strand Kit. Then, cDNA was mixed with RT^2 SYBR Green ROX qPCR Mastermix, loaded into the designated PCR array, and subjected to the following thermocycling parameters: 95°C for 10 min and then, 40 cycles of two-temperature PCR, 95°C for 15 s for denaturing, 60°C for 1 min for annealing and extension. Data analysis was conducted via web-based PCR array data software (http://sabiosciences.com/pcrarraydataanalysis.php) using the delta-delta Ct method with *HPRT1* and *RP13A* used as endogenous controls, since *ACTB, B2M,* and *GAPDH* expression were shown to be altered during spheroid formation [5]. Results are represented as the log of relative expression levels for each gene between the two samples plotted against each other in a Scatter Plot. Differential expression is represented as deviation away from the middle line $x = y$, represented on the graph. Deviation greater than 2-fold regulation is represented as a data point outside the exterior lines on the graph.

ELISA and cytokine array

MSC spheroids were prepared and cultured in hanging drops for 96 h in 4.5% FBS MEMα, as described above. The conditioned media was collected and secreted BMP2, IL1B, and leukemia inhibitory factor (LIF) were measured by quantitative ELISA kits according to each manufacturer's instruction (Bio-Techne for BMP2 and IL1B; eBioscience for LIF). The readouts were adjusted per μg of total cellular protein and 2D monolayer conditioned media was used as control.

Growth factors and cytokines within the conditioned media were also evaluated by Human Cytokine Antibody Array C5, a semi-quantitative, sandwich ELISA-based array (RayBiotech) according to manufacturer's instruction. In brief, after incubation with blocking buffer, conditioned media, prenormalized to total cellular protein, were incubated with the cytokine array membrane. After washing, the membrane was probed with biotin-conjugated antibodies followed by HRP-conjugated streptavidin for signal detection from the

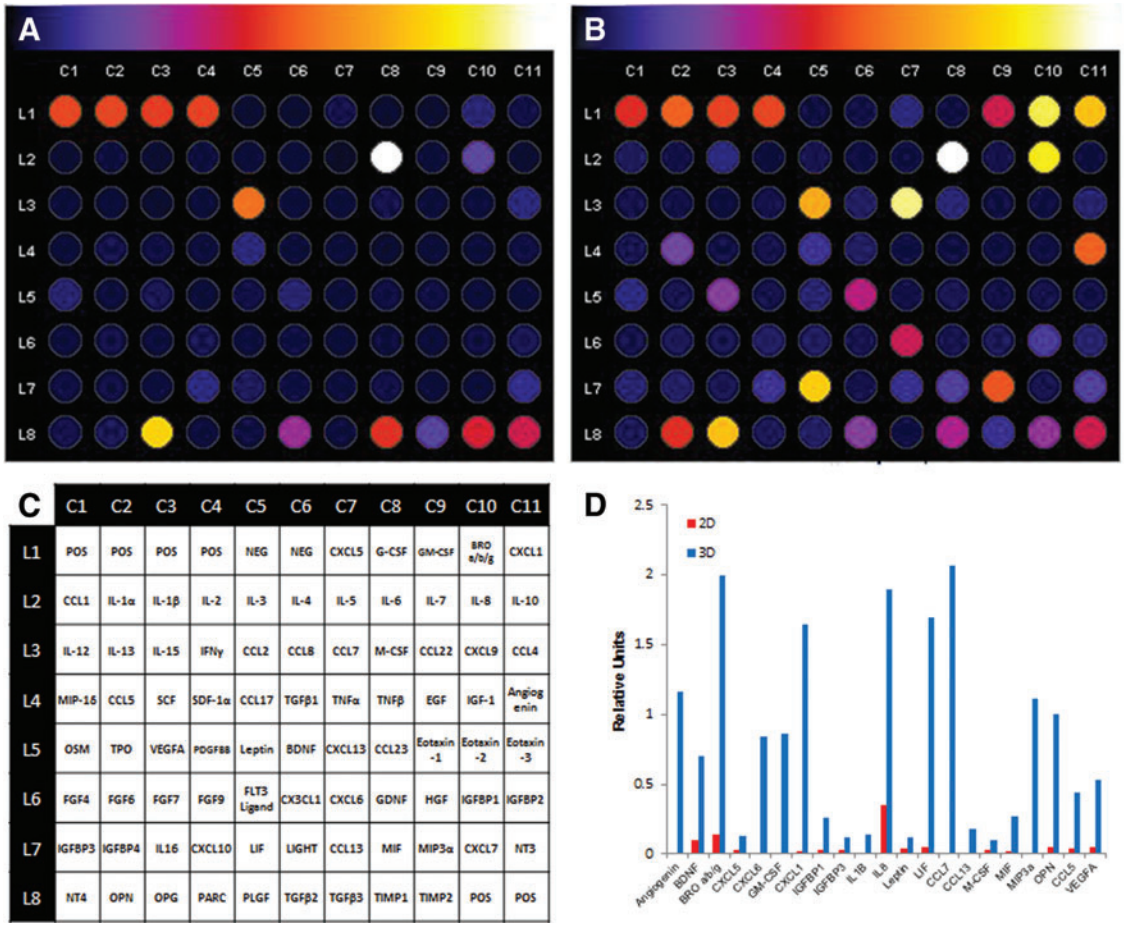

FIG. 2. Comparison of protein expression profile between 2D standard culture and 3D spheroidal culture by cytokine array. Conditioned medium was collected from MSC spheroids prepared via the hanging drop method after 96 h and analyzed using the Human Cytokine sandwich-based ELISA array. ImageJ analysis of 2D **(A)** and 3D **(B)** relative luminescent intensity is represented on a *blue* to *white* scale, as indicated above the panels. **(C)** Reference layout of Human Cytokine Array C5. **(D)** Summary plot of highly upregulated proteins in 3D spheroidal aggregates. Units relative to positive well controls (L1C1–L1C4, L8C10–L8C11). Color images available online at www.liebertpub.com/scd

membrane-bound cytokines. The chemiluminescent signal intensities were analyzed using the ImageJ Protein Array Analyzer Macro [Carpentier G. (2010), Protein Array Analyzer for ImageJ, http://rsb.info.nih.gov/ij/macros/toolsets/Protein Array Analyzer.txt] with intensities normalized to positive control wells across all samples.

Agar-encapsulation of MSC spheroids

Spheroids formed for 24 h in hanging drops were collected and suspended in 75 μL 1% agar-MEMα gel. Total RNA was collected using Plant mRNeasy Kit from Qiagen, as per manufacturer's instructions. cDNA synthesis and qRT-PCR proceeded as described above.

siRNA transient gene knockdown

Anti-BMP2 siRNA (SI00023359), anti-SMAD6 (SI03113425) siRNA, and Allstars Negative Control were purchased from Qiagen. Cells were transfected with 30 nM siRNA using HiPerfect Transfection reagent, according to manufacturer's instructions. For 3D siRNA knockdown, hMSCs were transfected for 24 h, then underwent spheroid formation. Total RNA was collected at 48 h post-spheroid formation.

Microarray data analysis

A Human Genome U133 Plus 2.0 chip (Affymetrix, Inc.) generated DNA microarray data set [12] was reanalyzed. Total RNA of hMSCs cultured in 2D monolayer or 3D spheroid was collected in triplicate. Data was manually set to a non-log scale and signals below a background threshold of 10 were eliminated, leaving 38,076 data points. Duplicated gene probes were consolidated into 19,321 genes by an online software Biobase ExPlain™ 3.1 Gene Expression Analysis System (Qiagen), to evaluate the upregulated (>2-fold) and downregulated (>2-fold) genes in MSC spheroids. The upregulated (>2-fold) and downregulated (>2-fold) genes in MSC spheroids were also analyzed by another online software Ingenuity Pathway Analysis (IPA) (Qiagen) to predict top upstream regulators for these upregulated and downregulated genes.

Cell survival assay

Equal number of cells was seeded in either 2D or 3D conditions, with or without exogenous BMP2 stimulation for 48 h. Cells were collected and mixed with XTT (ATCC) as per manufacturer's instructions. In brief, 50 μL of XTT

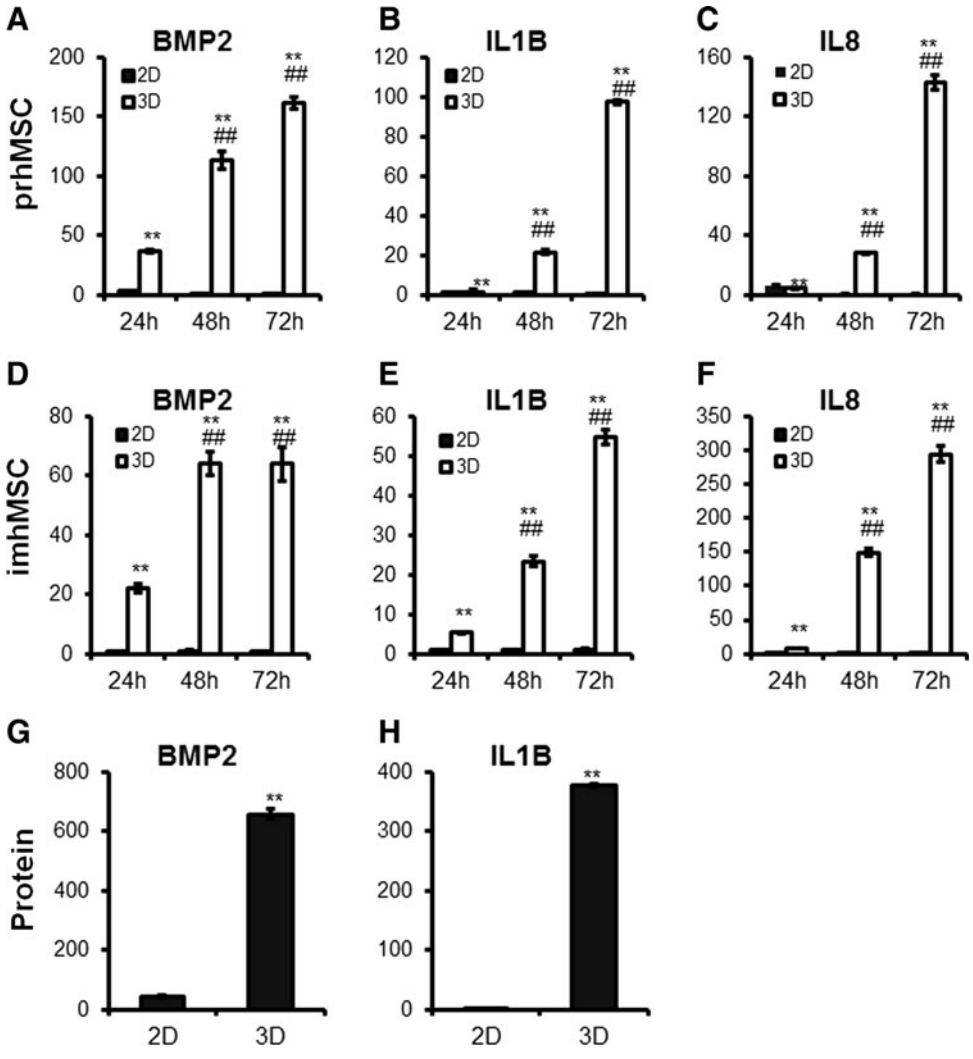

FIG. 3. Time course of *BMP2, IL1B,* and *IL8* expression during spheroid formation of MSCs. **(A–F)** Spheroidal aggregates of prhMSC **(A–C)** and imhMSC **(D–F)** were prepared via the hanging drop method and total RNA was harvested at the indicated time for gene expression analysis by qRT-PCR with TaqMan® primers. Values are given as the relative expression normalized to the 2D condition at 48 h. **(G, H)** prhMSC were cultured in either 2D or 3D handing drop conditions for 96 h and conditioned media were collected for ELISA analysis for BMP2 **(G)** and IL1B **(H)**. Values given are in pg/mL normalized to μg of cellular protein ($^{**}P < 0.005$ to control in 2D MSCs at 24 h, $^{\#\#}P < 0.005$ to 2D MSCs at the same time point). BMP, bone morphogenic protein; imhMSC, immortalized MSCs; prhMSC, primary MSCs; IL, interleukin.

solution was added to 100 μL of cells and incubated at normal growth conditions for 2 h. The light absorbance at 475 and 660 nm was read by a Synergy HT reader (Biotek). Specific light absorbance at 475 nm was calculated in reference to the light absorbance at 660 nm.

Statistical analysis

All experiments were performed in triplicate. Data were analyzed using Student *t*-test with significance set at $P < 0.05$ with lower *P*-values noted in figures and legends where appropriate.

Results

Dramatic change in gene expression profiles in 3D spheroidal culture

To understand the overall gene expression profile change in spheroidal aggregates of MSCs, we revisited a microarray gene expression data set already published earlier with ExPlain 3.1 and IPA software [12]. Among 19,321 genes, 10.2%, or 1,968 genes, including *BMP2*, *BMP6*, angiogenic factors (*VEGFA*), inflammatory cytokines (*IL1A*, *IL1B*, and *IL8*), IL6-class cytokines (*IL6*, *IL11*, and *LIF*), anti-inflammatory molecules (*PTGS2/COX2*, *TNFAIP6*, and *SOD2*), and chemokines

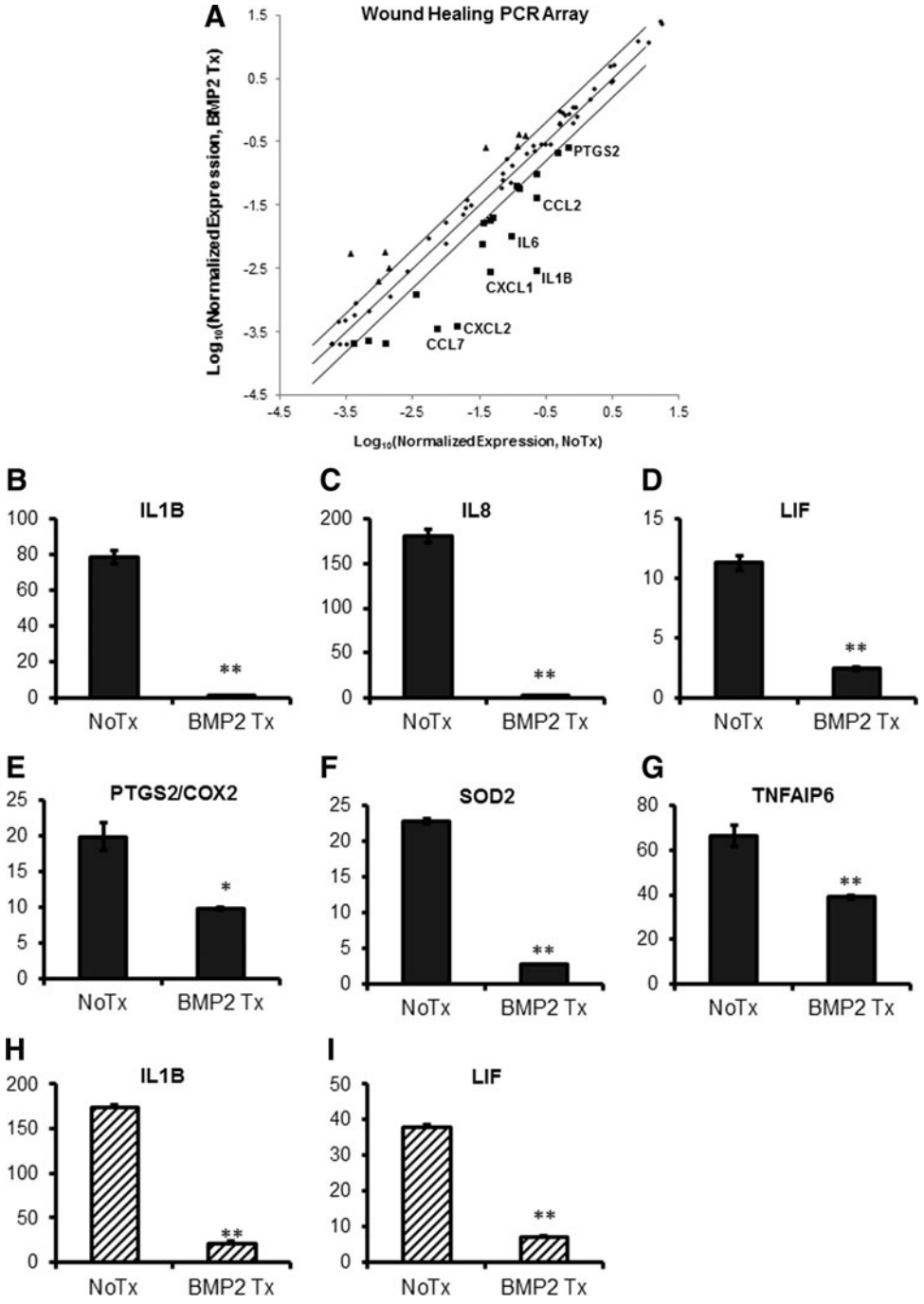

FIG. 4. BMP2 signaling downregulates gene expression of pro- and anti-inflammatory mediators and chemokines in MSC spheroids. MSC spheroids were prepared by using the hanging drop method in the presence of BMP2 (100 ng/mL) for 48 h and total RNA was harvested for gene expression analysis by Human Wound Healing PCR Array (Qiagen) **(A)**. The relative expression levels for each gene in the nontreated (*x*-axis) and BMP-treated (*y*-axis) samples are plotted against each other in the Scatter Plot. The upregulated genes (>2) are shown with *triangles*, whereas the downregulated genes (<0.5) are shown with *squares*. **(B–G)** mRNA expression was confirmed by qRT-PCR with TaqMan primers for *IL1B* **(B)**, *IL8* **(C)**, *LIF* **(D)**, *PTGS2/COX2* **(E)**, *SOD2* **(F)**, and *TNFAIP6* **(G)**. Values are given in fold-increase of nontreated MSCs in 2D standard condition. **(H–I)** Conditioned media were collected from MSC spheroids treated with BMP2 (100 ng/mL) after 96 h and analyzed with sandwich-based ELISAs for IL1B **(H)** and LIF **(I)**. Values given are in pg/mL (IL1B) and ng/mL (LIF) normalized to μg of cellular protein ($*P < 0.05$, $**P < 0.005$ to nontreated 3D MSC spheroids). LIF, leukemia inhibitory factor.

Table 3. Fold Change of Gene Expression by BMP2 Treatment in MSC Spheroids in Fig. 4

	Pro- and anti-inflammatory genes	
CCL2	Chemokine (C-C motif) ligand 2	–6.35
CCL7	Chemokine (C-C motif) ligand 7	–23.22
CXCL1	Chemokine (C-X-C motif) ligand 1	–17.72
CXCL2	Chemokine (C-X-C motif) ligand 2	–40.71
IL1B	Interleukin 1, beta	–88.49
IL6	Interleukin 6 (interferon, beta 2)	–10.68
PTGS2/ COX2	Prostaglandin-endoperoxide synthase 2/cyclooxygenase-2	–2.98

(*CXCL1* and *CXCL2)* were upregulated (>2-fold, top 50 upregulated genes in the microarray data are shown in bold); whereas 6.3%, or 1,223 genes, including extracellular matrix (ECM)/its regulatory molecules (*COL1A1*, *COL1A2*, and *CTGF)* and actin/its regulatory molecules (*ACTA2* and *ACTB*) were downregulated (>2-fold, top 50 downregulated genes in the microarray data are shown in bold) in MSC spheroids, consistent with previous studies [6,29]. These findings were confirmed by TaqMan-based qRT-PCR and PCR-arrays (Table 2 and Figs. 1 and 3). IPA analysis predicted IL1B as a top upstream regulator of the upregulated genes (*P*-value, 5.99×10^{-32}), consistent with the results in a previous study [15]. Gene expression changes were further verified using the Human Cytokine sandwich-based ELISA array for protein evaluation (Fig. 2).

Expression of BMP2 and IL1B is upregulated during MSC spheroid formation

The self-aggregation process of MSCs was shown to initiate caspase-dependent IL1 autocrine signaling [15]; however, upregulated IL1 signaling alone cannot account for the overall gene expression profile change in MSC spheroids. Moreover, the molecular pathways that initiate IL1 signaling in MSC spheroids remain unknown. To address this question, we first evaluated a time course of highly upregulated growth factors/cytokines (*BMP2*, *IL1B*, and *IL8*) during spheroid formation. Gene expression of *BMP2* and *IL1B* started rising around 24 h after hanging drop culture preparation. *BMP2* upregulation appeared

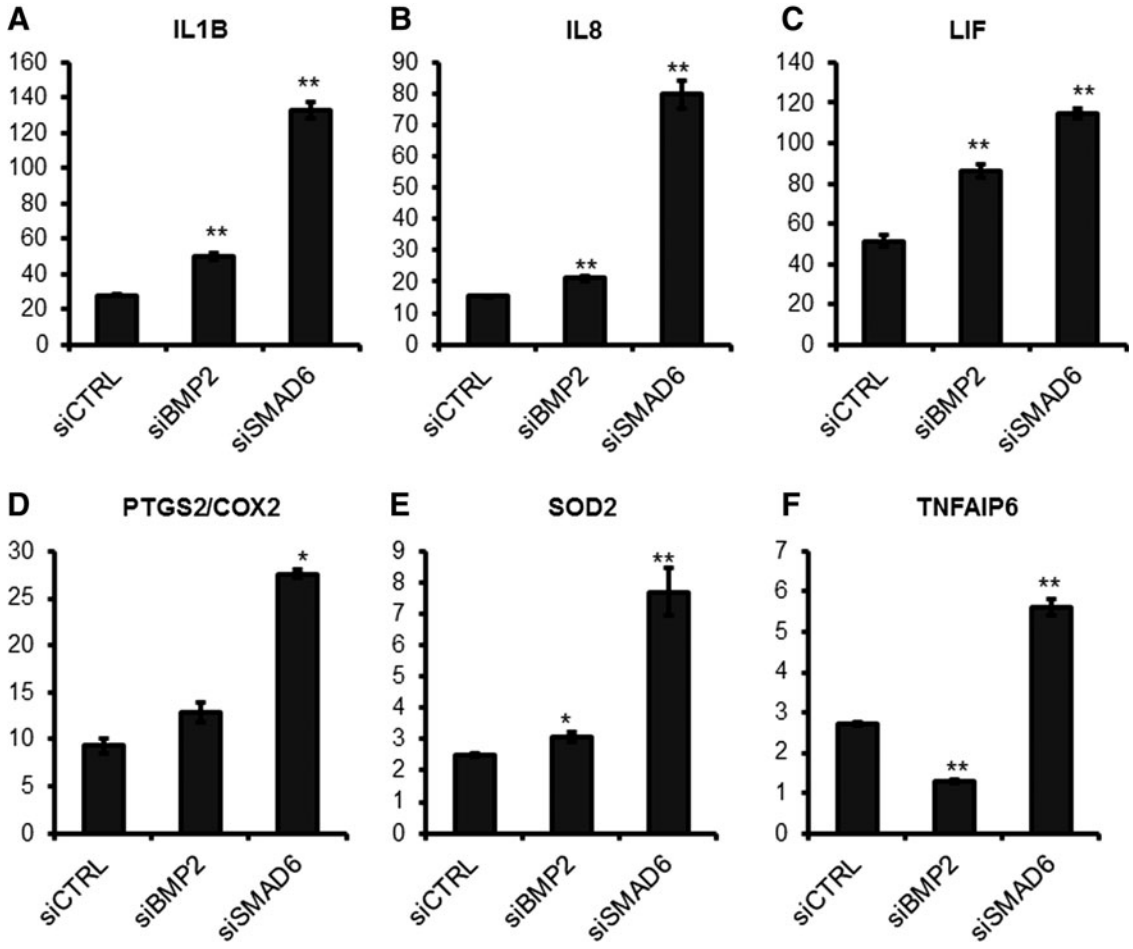

FIG. 5. siRNA-based knockdown of BMP2 or SMAD6 alters gene expression of pro- and anti-inflammatory mediators in MSC spheroids. **(A–F)** After 24 h of treatment with 30 nM of siCTRL, siBMP2, or siSMAD6, MSC spheroids were prepared using the hanging drop method and total RNA was harvested at 48 h after siRNA treatment for gene expression analysis by qRT-PCR with TaqMan primers. Values given are normalized to 2D MSC controls. The knockdown efficacy of BMP2 and SMAD6 was 76% and 89%, respectively (*$P < 0.05$, **$P < 0.005$ to siCTRL MSC spheroids). siCTRL, siRNA control; siBMP2, siRNA against BMP2; siSMAD6, siRNA against SMAD6.

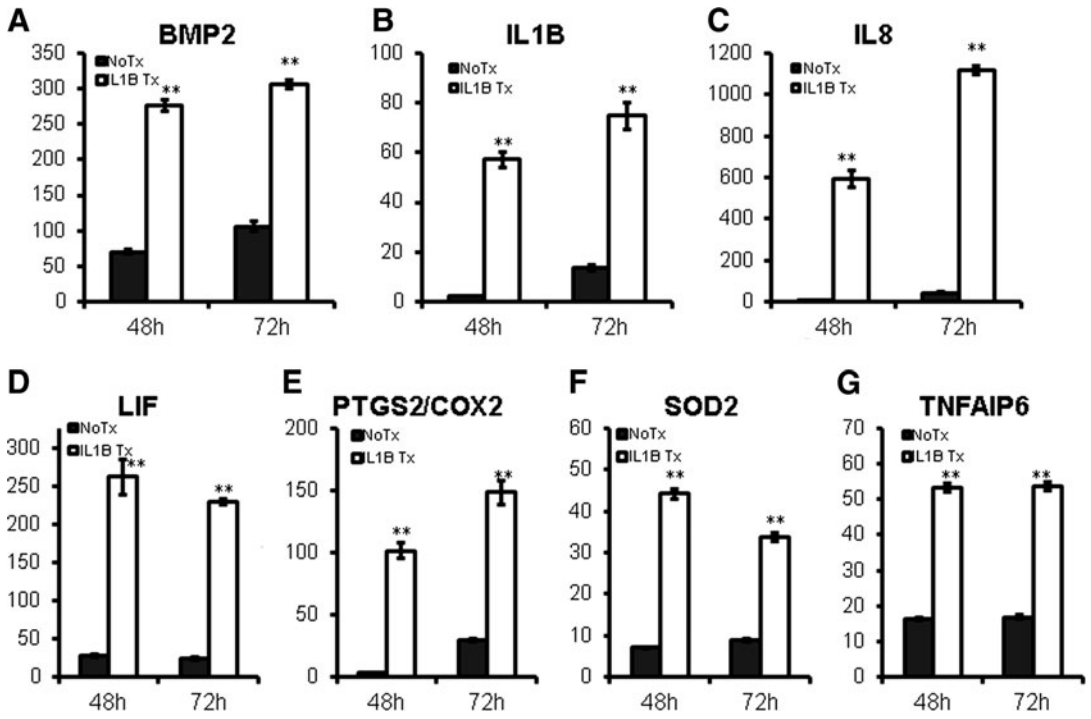

FIG. 6. IL1B signaling upregulates gene expression of pro- and anti-inflammatory mediators in MSC spheroids. **(A–G)** MSC spheroids were prepared by using the hanging drop method in the presence of IL1B (10 ng/mL) for 48 or 72 h and total RNA was harvested for gene expression analysis by qRT-PCR with TaqMan primers. Values are given in fold-increase of 2D condition at 24 h (**$P < 0.005$ to nontreated MSC spheroids at the same time point).

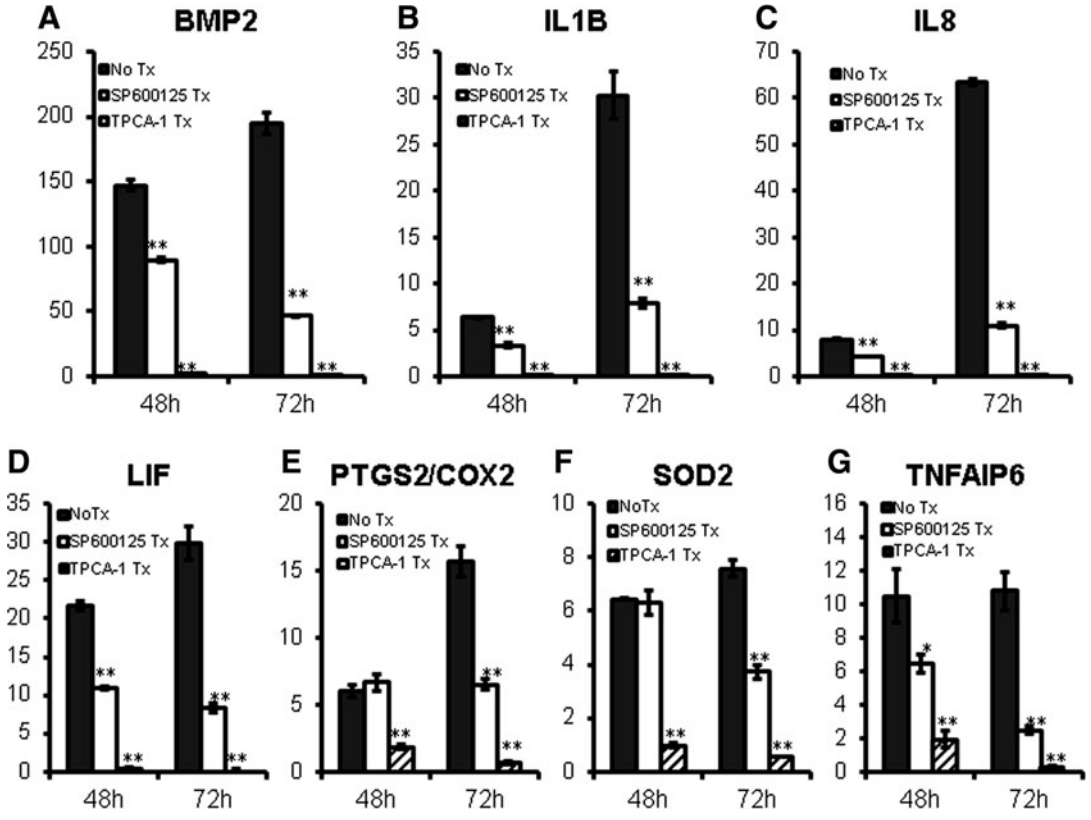

FIG. 7. Inhibition JNK or NFκB pathway reduces gene expression of pro- and anti-inflammatory mediators in MSC spheroids. **(A–G)** MSC spheroids were prepared by using the hanging drop method in the presence of JNK pathway inhibitor SP600125 (10 μM) or NFκB pathway inhibitor TPCA-1 (1 μM) for 48 or 72 h and total RNA was harvested for gene expression analysis by qRT-PCR with TaqMan primers. Values are given in fold-increase of 2D condition at 24 h (*$P < 0.05$, **$P < 0.005$ to nontreated MSC spheroids at the same time point).

earlier than that of *IL1B* expression (Fig. 3A, B, D, and E), indicating that *BMP2* upregulation is not a secondary event of IL1 signaling. *IL8* expression was upregulated in parallel with *IL1B* expression in MSCs (Fig. 3C, F). Protein expression of BMP2 and IL1B was evaluated by sandwich-based ELISA confirming the translation of gene expression upregulation to the protein expression (Fig. 3G, H).

BMP2 treatment strongly reduces proinflammatory and anti-inflammatory signaling in MSC spheroids

BMP2 is one of the highly upregulated genes in MSC spheroids (Table 2 and Fig. 1). Although physiological roles of BMP2 in MSCs have been extensively studied in the context of osteogenic differentiation [20], other roles of BMP2 signaling have not been investigated.

We queried whether BMP2 signaling is located upstream of IL1 signaling in MSC spheroids by stimulating MSC spheroids with exogenous BMP2. Contrary to expectations, BMP2 treatment decreased the expression of proinflammatory cytokines (*IL1B* and *IL8*), anti-inflammatory molecules (*PTGS2/COX2*, *TNFAIP6*, and *SOD2*), and chemokines (*CXCL1*, *CXCL2*, *CCL2*, and *CCL7*) in MSC spheroids, presumably through strong downregulation of *IL1B* expression (Fig. 4 and Table 3).

To our knowledge, BMP2 inhibition of proinflammatory cytokine expression has not been previously reported, but BMP7 signaling is shown to inhibit IL1R signaling [30–32] through SMAD6 and SMAD7, inhibitory Smads (I-Smads) [33–35] or JNK inhibition [36]. Because BMP2 and BMP7 share downstream signaling pathways, I-Smad involvement in BMP2 inhibition of proinflammatory cytokines and anti-inflammatory molecules was tested. siRNA-based knockdown of SMAD6 increased expression of proinflammatory cytokines and anti-inflammatory molecules that had been downregulated by BMP2 signaling (Fig. 5). Furthermore, BMP2 treatment upregulates *SMAD6* and *SMAD7* expression in MSC spheroids (data not shown). These data indicate that BMP2 signaling inhibits IL1R signaling via SMAD6 in MSC aggregates.

IL1B treatment induces expression of BMP2 and pro- and anti-inflammatory molecules

Next, we tested whether IL1 signaling alters gene expression of *BMP2* and pro- and anti-inflammatory molecules in MSC spheroids. Results showed that IL1B treatment further induced their expression (Fig. 6). NFκB and JNK MAPK pathways are major signaling pathways activated downstream of IL1R activation [37]. Treatment with an NFκB inhibitor (TPCA-1) or JNK inhibitor (SP600125) reduced *BMP2* and pro- and anti-inflammatory gene expression in MSC spheroids (Fig. 7), indicating that IL1R signaling enhances gene expression of these molecules via NFκB and JNK MAPK pathways.

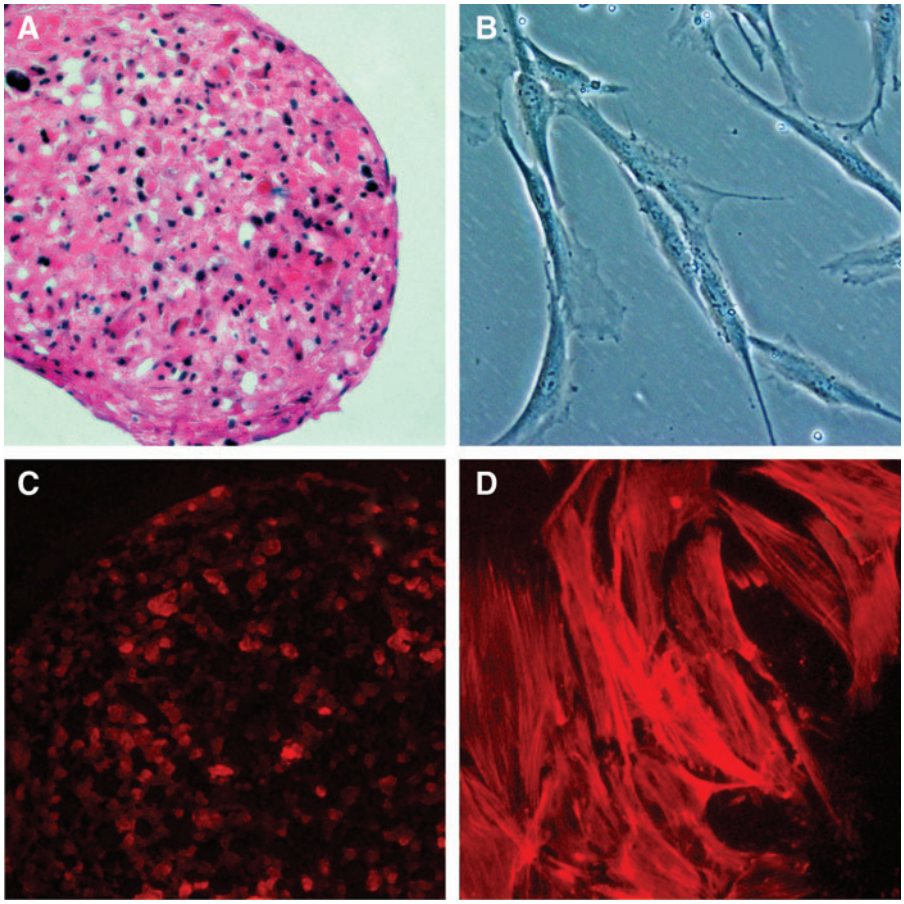

FIG. 8. Morphological differences of MSCs between the 3D spheroid culture and regular 2D culture. **(A)** H&E staining of MSC spheroid. **(B)** Cultured MSCs in monolayer under phase contrast. F-actin staining of MSC spheroid **(C)** and cultured MSCs in monolayer **(D)** with fluorescent phalloidin. Each photograph is 330 μm^2. Color images available online at www.liebertpub.com/scd

BMP2 is induced by soft elasticity-associated mechano-signaling

Individual cells in spheroidal aggregates had dramatic morphological differences (round shape and smaller size with less prominent F-actin) compared with MSCs in the 2D culture condition (Fig. 8), indicating a disparity in mechano-physical properties between these two conditions [5,38].

One major difference between 2D monolayer culture and 3D spheroid culture is the Young's elasticity modulus, or stiffness, of the materials surrounding the cells [39]; approximately a million-fold difference between the GPa range of a plastic surface for standard 2D culture and the approximately 0.1 kPa in 3D spheroidal cell aggregates [21]. Soft elasticity-associated mechano-signaling has been shown to alter gene expression and affect cell differentiation [22] leading to our hypothesis that soft elasticity-associated mechano-signaling initiates the gene expression change in the early phase of spheroid formation, especially before IL1B upregulation.

MSCs were cultured on soft elasticity culture plates with 200 Pa surfaces in a low serum condition to mimic the elasticity modulus and nutrient-limited microenvironment within spheroidal aggregates [5]. Soft elasticity-associated mechano-signaling caused moderate upregulation of *BMP2* and minimal induction of pro- and anti-inflammatory genes (*IL1B*, *IL8*, *PTGS2*, and *SOD2*); however, upon exogenous IL1B stimulation, elasticity-associated signaling amplifies the induction of these downstream genes (Fig. 9).

To further explore the role of the elasticity-associated signaling in MSC spheroids, we encapsulated MSC spheroids within a 1% agar gel (approximate to 13 kPa [40]) to directly manipulate the elasticity modulus of the spheroidal aggregates. Agar gel encapsulation decreased not only *BMP2* expression, but also that of pro- and anti-inflammatory genes (*IL1B*, *IL8*, *TNFAIP6*, *PTGS2/COX2*, and *SOD2*) (Fig. 10), further validating the importance of elasticity-associated signaling in MSC spheroids.

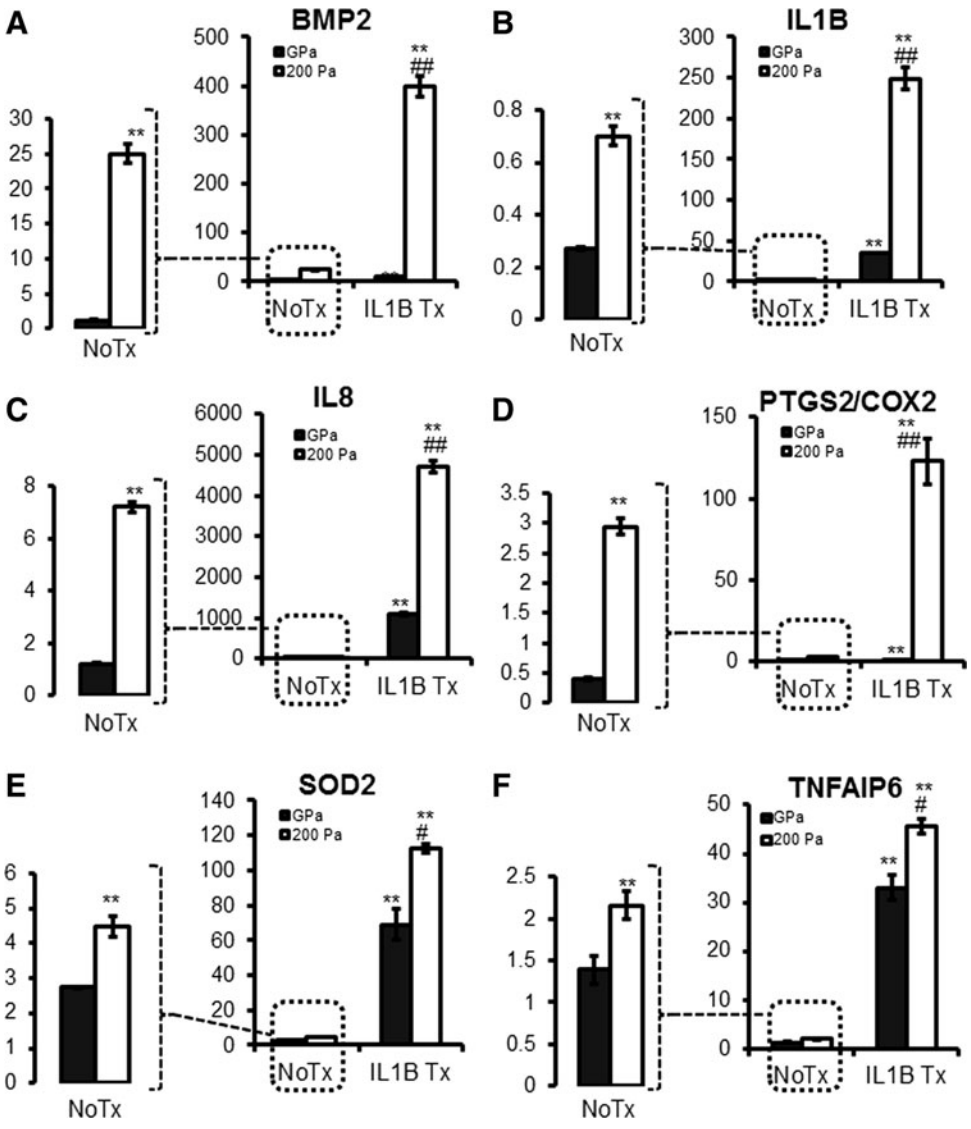

FIG. 9. Soft elasticity mechano-signaling induces BMP2 expression both independently and synergistically with IL1B treatment. **(A–F)** MSCs were cultured in MEMα with 0.1% FBS on either a standard plastic cell culture surface (GPa) or low elasticity cell culture surface (200 Pa) coated with type I collagen in the presence or absence of IL1B (10 ng/mL), and total RNA was harvested for gene expression analysis by qRT-PCR with TaqMan primers. Values are given in fold-increase of MSCs cultured in standard culture conditions (MEMα with 17% FBS and standard plastic cell culture plate). No Treatment (No Tx) conditions are enlarged to highlight the effect of soft elasticity-associated mechano-signaling [$^{**}P < 0.005$ to NoTx on GPa, $^{\#}P < 0.05$, $^{\#\#}P < 0.005$ to IL1B treatment (IL1B Tx) on GPa]. MEMα, minimal essential medium α.

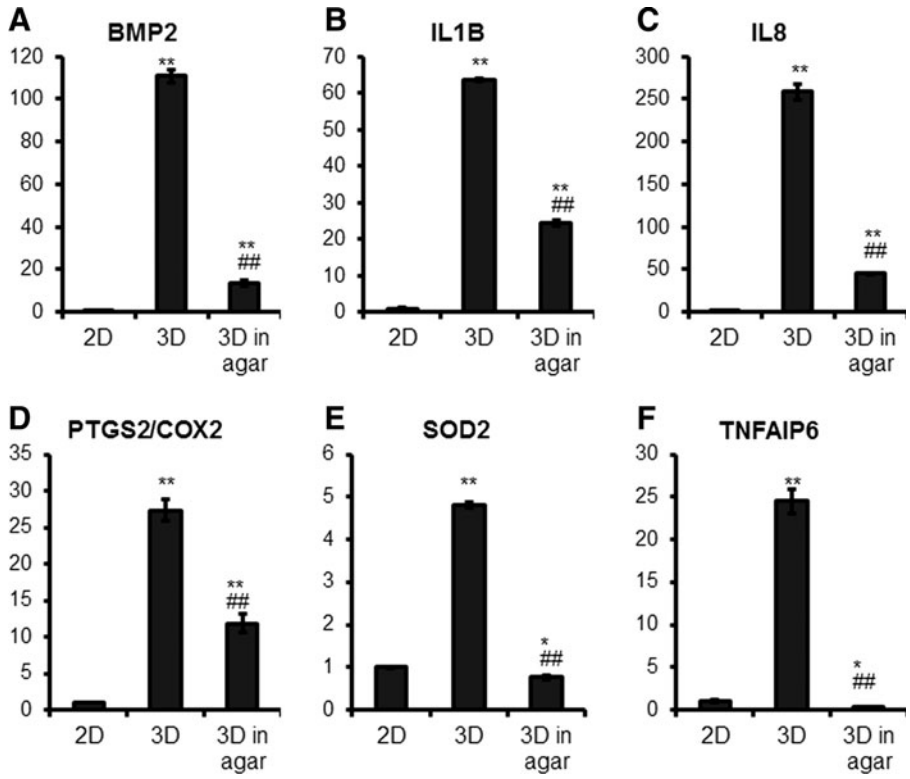

FIG. 10. Applied stiffness reduces gene expression of pro- and anti-inflammatory mediators in spheroid aggregates. **(A–F)** MSCs were cultured in hanging drops to form spheroid aggregates for 24 h, then suspended in a 1% agar gel for 48 h. Standard 2D culture and non-agar embedded spheroid aggregates were used as controls. Total RNA was harvested for gene expression analysis by qRT-PCR with TaqMan primers. Values are given as relative expression normalized to the 2D culture condition ($*P < 0.05$, $**P < 0.005$ to 2D condition, $^{\#\#}P < 0.005$ to 3D condition).

BMP2 signaling enhances cell survival and cell spreading of MSC spheroids

Disassembly and spreading of spheroidal aggregates is expected to happen after transplantation into the body. Similarly in vitro, once MSC spheroids are placed on an ECM surface, spheroidal aggregates start spreading and adhering to the surface. These spheroid-derived MSCs, or individual cells dissociated from 3D spheroidal culture, are more resistant to cytotoxic stimuli than MSCs maintained in the regular 2D condition [7]; however, MSCs within the aggregates are more vulnerable to H_2O_2 stress (Fig. 11). BMP2 treatment improved cell viability within spheroids and promoted rapid disassembly and spreading of spheroids (Figs. 11 and 12), indicating that BMP2 signaling provides a survival advantage to MSC spheroids soon after transplantation, which is expected to improve therapeutic efficacy.

Discussion

In this article, we showed that (1) BMP2 and proinflammatory cytokines (IL1B and IL8) are upregulated during spheroid formation (Figs. 1–3); (2) BMP2 signaling is inhibitory for pro- and anti-inflammatory mediator induction (Figs. 4 and 5); (3) IL1 signaling is stimulatory for BMP2 and pro- and anti-inflammatory mediator induction (Figs. 6 and 7); (4) soft elasticity-associated mechano-signaling elevates BMP2 expression and enhances IL1 signaling (Figs. 8–10); and (5) BMP2 signaling enhances cell survival and cell spreading of MSC spheroids (Figs. 11 and 12). Our proposed model of BMP and IL1 signaling in MSC spheroids is included in Fig. 13. The overall therapeutic effects of MSC spheroids are expected to be enhanced by either targeting BMP2 itself or BMP2 downstream effector molecules, resulting in new approaches for maximizing MSC-based therapeutics.

As described in the introduction and results sections, our original motivation of this study was to learn the underlying molecular mechanisms of the dramatic gene expression profile change in MSC spheroids. We initially hypothesized that BMP2 upregulation initiates IL1 signal self-activation in MSC spheroids because time course data showed that *BMP2*

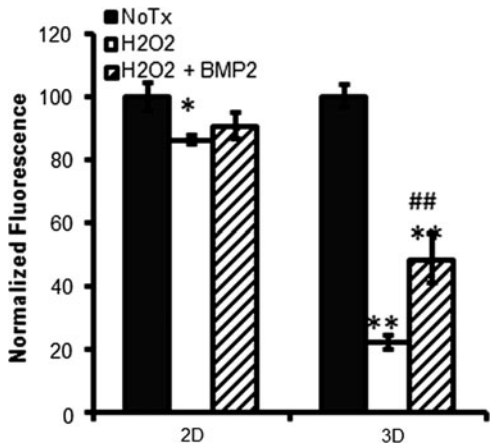

FIG. 11. BMP2 treatment improves cell viability in H_2O_2-vulnerable MSC spheroids. MSC spheroids were prepared by using hanging drop method in the presence or absence of BMP2 (100 ng/mL) for 48 h, then cells were treated with H_2O_2 (300 μM) for 4 h and the cell viability was assessed by XTT assay. Values of nontreated (No Tx) controls in each condition (2D or 3D) were normalized to 100% ($*P < 0.05$, $**P < 0.005$ to No Tx, $^{\#\#}P < 0.005$ to H_2O_2-treated group).

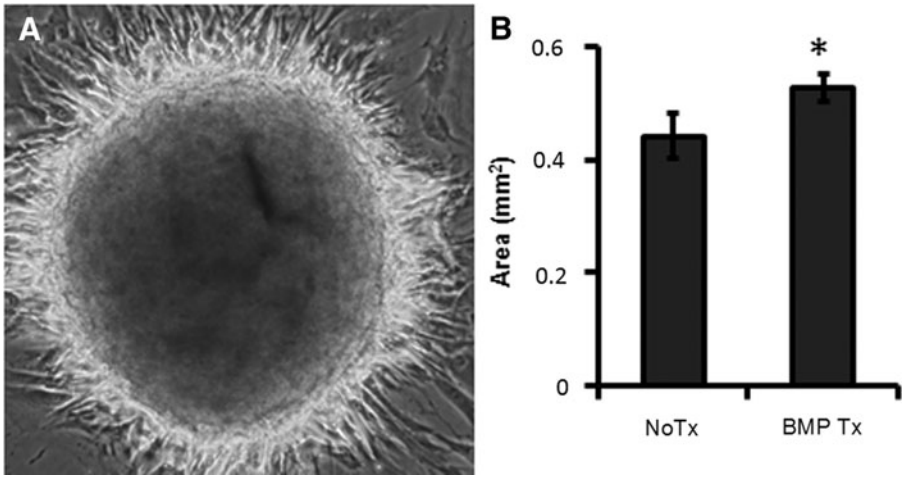

FIG. 12. BMP2 signaling promotes spreading of MSC spheroids. MSC spheroids were prepared by using the hanging drop method in the presence of BMP2 (100 ng/mL) for 48 h, then plated on collagen-coated cell culture plates. **(A)** A representative image (550 μm^2) of MSC spheroid attachment at 24 h after seeding. **(B)** The total area (mm^2) of spreading at 48 h [$^*P < 0.05$, to nontreated (No Tx) MSC spheroids].

upregulation takes place before that of IL1B and IL8 during spheroid formation (Fig. 3) and a previous study showed that BMP2 signaling activates caspases in osteoblasts [41].

To our surprise, BMP2 signaling inhibits IL1 signaling and subsequent pro- and anti-inflammatory mediator induction via SMAD6 in MSC spheroid. SMAD6 is an inhibitory Smad that inhibits canonical Smad signaling; however, we speculate that SMAD6-mediated inhibition of canonical Smad is not a major mechanism of BMP2 inhibition of pro- and anti-inflammatory signaling since SMAD6 knockdown reverses the effect of BMP2 signaling (Fig. 5).

Previous studies have shown that BMP7 signaling inhibits IL1R/TLR signaling [30,32,33,42] through I-Smads [33–35]. SMAD6 interferes with IL-1R-associated kinase 1 (IRAK1)-mediated signaling by interacting with Pellino-1 [34,35] or Smad ubiquitin regulator factor protein (Smurf) E3 ligase [33]. Pellino-1 is an adaptor molecule of IRAK1 that mediates IL1R/TLR and NFKb in the downstream of MyD88, whereas Smurf E3 ligase is targeting MyD88. Thus, we speculate that Pellino-1 and/or Smurf E3 might mediate the inhibitory effect of BMP2 signaling in MSC spheroids; however, further studies about the roles of Pellino-1 and/or Smurf E3 ligase are beyond the scope of this article.

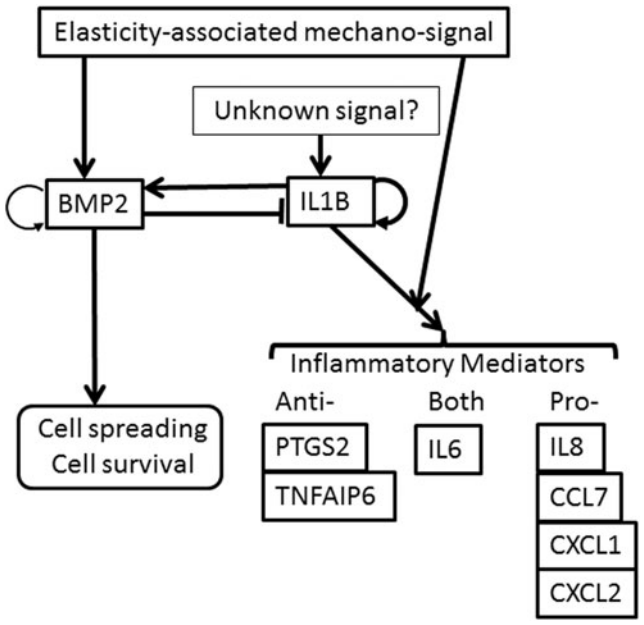

FIG. 13. Proposed model of BMP and IL1 signaling in MSC spheroids.

BMP2 has been extensively studied in MSC biology in the context of osteogenesis or osteoblastic differentiation [20]. BMP2 signaling is osteogenic for MSCs cultured on a stiff surface, but not osteogenic on a soft elasticity surface due to a decrease in R-Smad phosphorylation and subsequent nuclear translocation [42,43]. Thus, even though BMP2 expression is upregulated in MSC spheroids, we speculate that it is not necessarily osteogenic for MSCs within spheroidal aggregates. Further support of the lack of osteoblastic differentiation in spheroids is the lack of upregulation of *RUNX2*, a key osteogenic factor, at least during our observation up to 72 h after spheroid formation (data not shown). The cells within spheroidal aggregates might be able to undergo osteogenic lineage, however, in the presence of concurrent signals that permit osteogenesis, such as stiff surface-associated signaling.

What is the physiological significance of upregulated BMP signaling in MSC spheroids? BMP signaling induces the regenerative response through blastema formation, presumably by reactivating tissue development programs [18,44]. As in vivo counterpart of MSC spheroids is presumably blastema or blastemal-like structure and formation of blastema is a key regeneration step in amphibians (and mammalian though in a limited degree) [14,19], this upregulation of BMP signaling might recapitulate the blastema-mediated regeneration process in the body.

It is puzzling that even in the presence of strong BMP2 upregulation, the equilibrium between BMP2 and IL1 signaling is IL1 dominant. MSCs require proinflammtory cytokine stimulation to acquire anti-inflammatory or immunomodulatory properties [45], so this dominant IL1 signaling confers anti-inflammatory properties to MSC spheroids. It is also unclear why the effects of siRNA-based knockdown of BMP2 are relatively weak (Fig. 5), compared with the effects of SMAD6 knockdown. As BMP6 is also upregulated in MSC spheroids (Fig. 1), the two molecules may compensate for each other. Double-knockdown of BMP2 and BMP6 in MSC spheroids would test this speculation, but it is beyond the scope of this article.

By using a soft elasticity cell culture surface with 200 Pa, we showed that elasticity-associated signaling elevates BMP2

expression and enhances IL1 signaling in MSCs. These results are consistent with the experimental results of direct modulation of stiffness, in which encapsulation of MSC spheroids with 1% agar (approximate to 13 kPa [40]) downregulates gene expression of *BMP2*, *IL1B*, and other pro- and anti-inflammatory mediator genes (Fig. 9). The 1% agar should not affect diffusion of nutrients and protein [46]; thus, it is highly unlikely to cause accumulation of growth factors and cytokines produced by MSC spheroids. Concurrent downregulation of BMP2 and IL1 signaling can be explained by elasticity-mediated signaling enhancement of IL1 signaling being stronger than BMP2 inhibition of IL1 signaling in MSC spheroids. These results clearly show the importance of elasticity-associated signaling in MSC spheroids.

The upstream molecular events of IL1 signal self-activation in MSC spheroids is still uncertain. Activation of the JNK pathway in the cells within spheroidal aggregates (Fig. 7) is consistent with cellular stress due to limited O_2 and nutrient diffusion [5]. Even though the combination of these stressors (mimicked by serum-starved culture condition) and soft elasticity-associated mechano-signaling enhances IL1 signaling, it does not initiate IL1 signaling (Fig. 9).

The question remains: should BMP2 signaling be maximized or inhibited in MSC spheroids? BMP2 signaling reduces anti-inflammatory effects of MSC spheroids, but it also reduces their proinflammatory effects. Our study indicates that BMP2 signaling provides a survival advantage for MSC spheroids (Figs. 11 and 12), but further studies are needed to address further roles of BMP2 signaling in MSC spheroids. Then, either BMP2 agonist or antagonist could be used to maximize the therapeutic effects of MSC spheroids.

In summary, we showed the significance of soft elasticity-associated mechano-signaling and BMP2 signaling in MSC spheroids. This research advances basic knowledge about MSC biology and the 3D culture system.

Acknowledgments

This study was supported by the University of Pittsburgh Schools of Health Sciences (Bridge Funding Category One), University of Pittsburgh Medical Center Health System (Competitive Medical Research Fund), and departmental funds (Department of Pathology, University of Pittsburgh School of Medicine) (to K.T.) and University of Pittsburgh School of Medicine Summer Undergraduate Research Program (SURP) (to J.F.). We would like to thank Dr. Junya Toguchida (Kyoto University, Kyoto, Japan) for his kind gift of immortalized human MSCs and Ms. Jonette V. Werley (Division of Neuropathology, Department of Pathology, University of Pittsburgh School of Medicine) for her technical support. We would also thank Drs. James Wang, Harry Blair, and Carry Wu (University of Pittsburgh) and Dr. Adam W. Feinberg (Carnegie Mellon University) for their insightful discussion.

Author Disclosure Statement

No competing financial interests exist.

References

1. Caplan AI. (2009). Why are MSCs therapeutic? New data: new insight. J Pathol 217:318–324.
2. Tamama K and DJ Barbeau. (2012). Early growth response genes signaling supports strong paracrine capability of mesenchymal stem cells. Stem Cells Int 2012:428403.
3. Tamama K and SS Kerpedjieva. (2012). Acceleration of wound healing by multiple growth factors and cytokines secreted from multipotential stromal cells/mesenchymal stem cells (MSCs). Adv Wound Care 1:177–182.
4. Tamama K, J Guan and K McFadden. (2016). Improving stem and progenitor cell therapeutics. Stem Cells Int 2016:1409762.
5. Cesarz Z and K Tamama. (2016). Spheroid culture of mesenchymal stem cells. Stem Cells Int 2016:9176357.
6. Bartosh TJ, JH Ylostalo, A Mohammadipoor, N Bazhanov, K Coble, K Claypool, RH Lee, H Choi and DJ Prockop. (2010). Aggregation of human mesenchymal stromal cells (MSCs) into 3D spheroids enhances their antiinflammatory properties. Proc Natl Acad Sci USA 107:13724–13729.
7. Cheng NC, SY Chen, JR Li and TH Young. (2013). Short-term spheroid formation enhances the regenerative capacity of adipose-derived stem cells by promoting stemness, angiogenesis, and chemotaxis. Stem Cells Transl Med 2:584–594.
8. Guo L, J Ge, Y Zhou, S Wang, RC Zhao and Y Wu. (2014). Three-dimensional spheroid-cultured mesenchymal stem cells devoid of embolism attenuate brain stroke injury after intra-arterial injection. Stem Cells Dev 23:978–989.
9. Hutton DL, EM Moore, JM Gimble and WL Grayson. (2013). Platelet-derived growth factor and spatiotemporal cues induce development of vascularized bone tissue by adipose-derived stem cells. Tissue Eng Part A 19:2076–2086.
10. Cerwinka WH, SM Sharp, BD Boyan, HE Zhau, LW Chung and C Yates. (2012). Differentiation of human mesenchymal stem cell spheroids under microgravity conditions. Cell Regen (Lond) 1:2.
11. Guo L, Y Zhou, S Wang and Y Wu. (2014). Epigenetic changes of mesenchymal stem cells in three-dimensional (3D) spheroids. J Cell Mol Med 18:2009–2019.
12. Potapova IA, GR Gaudette, PR Brink, RB Robinson, MR Rosen, IS Cohen and SV Doronin. (2007). Mesenchymal stem cells support migration, extracellular matrix invasion, proliferation, and survival of endothelial cells in vitro. Stem Cells 25:1761–1768.
13. Lund AW, B Yener, JP Stegemann and GE Plopper. (2009). The natural and engineered 3D microenvironment as a regulatory cue during stem cell fate determination. Tissue Eng Part B Rev 15:371–380.
14. Pennock R, E Bray, P Pryor, S James, P McKeegan, R Sturmey and P Genever. (2015). Human cell dedifferentiation in mesenchymal condensates through controlled autophagy. Sci Rep 5:13113.
15. Bartosh TJ, JH Ylostalo, N Bazhanov, J Kuhlman and DJ Prockop. (2013). Dynamic compaction of human mesenchymal stem/precursor cells into spheres self-activates caspase-dependent IL1 signaling to enhance secretion of modulators of inflammation and immunity (PGE2, TSG6, and STC1). Stem Cells 31:2443–2456.
16. Tsai AC, Y Liu, X Yuan and T Ma. (2015). Compaction, fusion, and functional activation of three-dimensional human mesenchymal stem cell aggregate. Tissue Eng Part A 21:1705–1719.
17. Reddi AH. (1997). Bone morphogenetic proteins: an unconventional approach to isolation of first mammalian morphogens. Cytokine Growth Factor Rev 8:11–20.

18. Yu L, M Han, M Yan, EC Lee, J Lee and K Muneoka. (2010). BMP signaling induces digit regeneration in neonatal mice. Development 137:551–559.
19. Muneoka K, CH Allan, X Yang, J Lee and M Han. (2008). Mammalian regeneration and regenerative medicine. Birth Defects Res C Embryo Today 84:265–280.
20. Zhang X, J Guo, Y Zhou and G Wu. (2014). The roles of bone morphogenetic proteins and their signaling in the osteogenesis of adipose-derived stem cells. Tissue Eng Part B Rev 20:84–92.
21. Baraniak PR, MT Cooke, R Saeed, MA Kinney, KM Fridley and TC McDevitt. (2012). Stiffening of human mesenchymal stem cell spheroid microenvironments induced by incorporation of gelatin microparticles. J Mech Behav Biomed Mater 11:63–71.
22. Engler AJ, S Sen, HL Sweeney and DE Discher. (2006). Matrix elasticity directs stem cell lineage specification. Cell 126:677–689.
23. Okamoto T, T Aoyama, T Nakayama, T Nakamata, T Hosaka, K Nishijo, T Nakamura, T Kiyono and J Toguchida. (2002). Clonal heterogeneity in differentiation potential of immortalized human mesenchymal stem cells. Biochem Biophys Res Commun 295:354–361.
24. Kawasaki H, J Guan and K Tamama. (2010). Hydrogen gas treatment prolongs replicative lifespan of bone marrow multipotential stromal cells in vitro while preserving differentiation and paracrine potentials. Biochem Biophys Res Commun 397:608–613.
25. Tamama K, VH Fan, LG Griffith, HC Blair and A Wells. (2006). Epidermal growth factor as a candidate for ex vivo expansion of bone marrow-derived mesenchymal stem cells. Stem Cells 24:686–695.
26. Foty R. (2011). A simple hanging drop cell culture protocol for generation of 3D spheroids. J Vis Exp pii:2720.
27. Barbeau DJ, KT La, DS Kim, SS Kerpedjieva, GV Shurin and K Tamama. (2014). Early growth response-2 signaling mediates immunomodulatory effects of human multipotential stromal cells. Stem Cells Dev 23:155–166.
28. Kerpedjieva SS, DS Kim, DJ Barbeau and K Tamama. (2012). EGFR ligands drive multipotential stromal cells to produce multiple growth factors and cytokines via early growth response-1. Stem Cells Dev 21:2541–2551.
29. Yeh HY, BH Liu, M Sieber and SH Hsu. (2014). Substrate-dependent gene regulation of self-assembled human MSC spheroids on chitosan membranes. BMC Genomics 15:10.
30. Bobacz K, IG Sunk, JG Hofstaetter, L Amoyo, CD Toma, S Akira, T Weichhart, M Saemann and JS Smolen. (2007). Toll-like receptors and chondrocytes: the lipopolysaccharide-induced decrease in cartilage matrix synthesis is dependent on the presence of toll-like receptor 4 and antagonized by bone morphogenetic protein 7. Arthritis Rheum 56:1880–1893.
31. Kaiser M, J Haag, S Soder, B Bau and T Aigner. (2004). Bone morphogenetic protein and transforming growth factor beta inhibitory Smads 6 and 7 are expressed in human adult normal and osteoarthritic cartilage in vivo and are differentially regulated in vitro by interleukin-1beta. Arthritis Rheum 50:3535–3540.
32. Gould SE, M Day, SS Jones and H Dorai. (2002). BMP-7 regulates chemokine, cytokine, and hemodynamic gene expression in proximal tubule cells. Kidney Int 61:51–60.
33. Lee YS, JS Park, JH Kim, SM Jung, JY Lee, SJ Kim and SH Park. (2011). Smad6-specific recruitment of Smurf E3 ligases mediates TGF-beta1-induced degradation of MyD88 in TLR4 signalling. Nat Commun 2:460.
34. Lee YS, JH Kim, ST Kim, JY Kwon, S Hong, SJ Kim and SH Park. (2010). Smad7 and Smad6 bind to discrete regions of Pellino-1 via their MH2 domains to mediate TGF-beta1-induced negative regulation of IL-1R/TLR signaling. Biochem Biophys Res Commun 393:836–843.
35. Choi KC, YS Lee, S Lim, HK Choi, CH Lee, EK Lee, S Hong, IH Kim, SJ Kim and SH Park. (2006). Smad6 negatively regulates interleukin 1-receptor-Toll-like receptor signaling through direct interaction with the adaptor Pellino-1. Nat Immunol 7:1057–1065.
36. Lee MJ, CW Yang, DC Jin, YS Chang, BK Bang and YS Kim. (2003). Bone morphogenetic protein-7 inhibits constitutive and interleukin-1 beta-induced monocyte chemoattractant protein-1 expression in human mesangial cells: role for JNK/AP-1 pathway. J Immunol 170:2557–2563.
37. O'Neill LA. (2000). The interleukin-1 receptor/Toll-like receptor superfamily: signal transduction during inflammation and host defense. Sci STKE 2000:re1.
38. Sart S, AC Tsai, Y Li and T Ma. (2014). Three-dimensional aggregates of mesenchymal stem cells: cellular mechanisms, biological properties, and applications. Tissue Eng Part B Rev 20:365–380.
39. Murphy WL, TC McDevitt and AJ Engler. (2014). Materials as stem cell regulators. Nat Mater 13:547–557.
40. Ahearne M, Y Yang, AJ El Haj, KY Then and KK Liu. (2005). Characterizing the viscoelastic properties of thin hydrogel-based constructs for tissue engineering applications. J R Soc Interface 2:455–463.
41. Hay E, J Lemonnier, O Fromigue and PJ Marie. (2001). Bone morphogenetic protein-2 promotes osteoblast apoptosis through a Smad-independent, protein kinase C-dependent signaling pathway. J Biol Chem 276:29028–29036.
42. Du J, X Chen, X Liang, G Zhang, J Xu, L He, Q Zhan, XQ Feng, S Chien and C Yang. (2011). Integrin activation and internalization on soft ECM as a mechanism of induction of stem cell differentiation by ECM elasticity. Proc Natl Acad Sci USA 108:9466–9471.
43. Zouani OF, J Kalisky, E Ibarboure and MC Durrieu. (2013). Effect of BMP-2 from matrices of different stiffnesses for the modulation of stem cell fate. Biomaterials 34:2157–2166.
44. Beck CW, B Christen, D Barker and JM Slack. (2006). Temporal requirement for bone morphogenetic proteins in regeneration of the tail and limb of Xenopus tadpoles. Mech Dev 123:674–688.
45. Krampera M. (2011). Mesenchymal stromal cell ''licensing'': a multistep process. Leukemia 25:1408–1414.
46. Pluen A, PA Netti, RK Jain and DA Berk. (1999). Diffusion of macromolecules in agarose gels: comparison of linear and globular configurations. Biophys J 77:542–552.

Address correspondence to:
Kenichi Tamama, MD, PhD, FCAP
Department of Pathology
University of Pittsburgh School of Medicine
3550 Terrace Street
S737 Scaife Hall
Pittsburgh, PA 15261

E-mail: tamamakj@upmc.edu

Received for publication November 15, 2015
Accepted after revision February 25, 2016
Prepublished on Liebert Instant Online February 26, 2016